

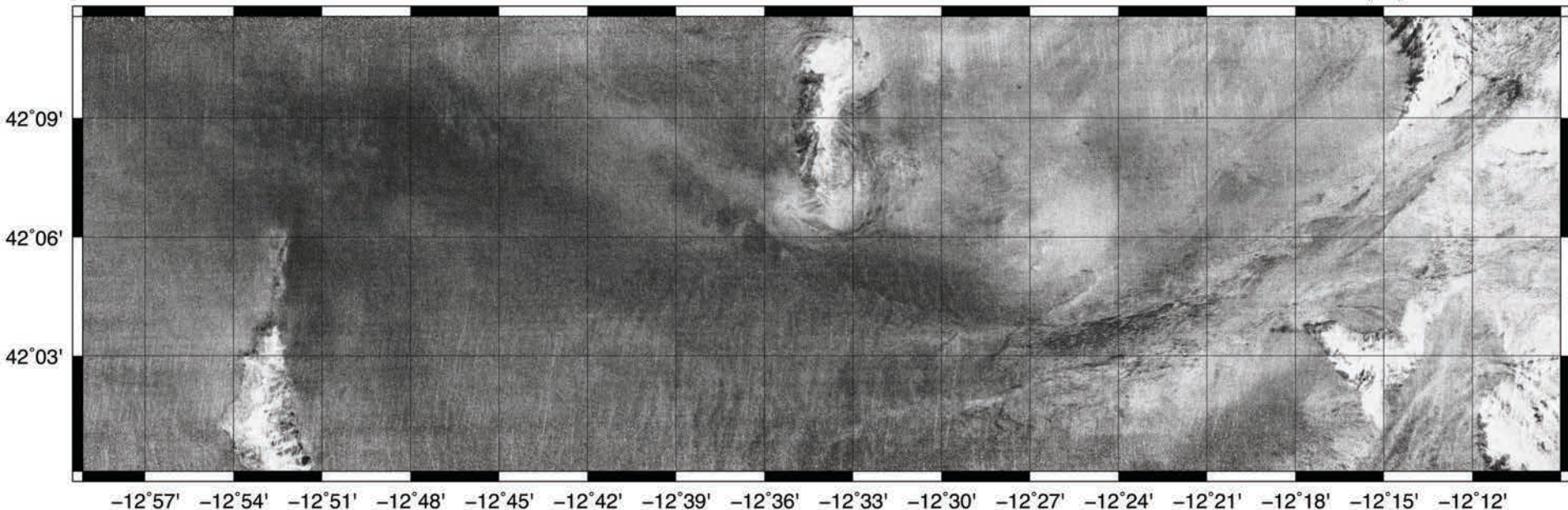
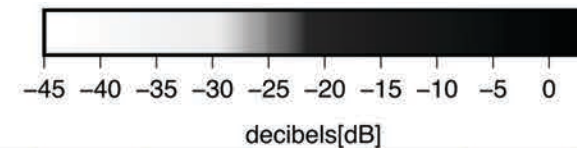
# Seafloor surface processes and subsurface paleo-channel unconformities mapped using multi-channel seismic and multi-beam sonar data from the Galicia 3D seismic experiment.

James Gibson, Donna Shillington, Dale Sawyer, Brian Jordan, Julia Morgan,  
Cesar Ranero, and Tim Reston

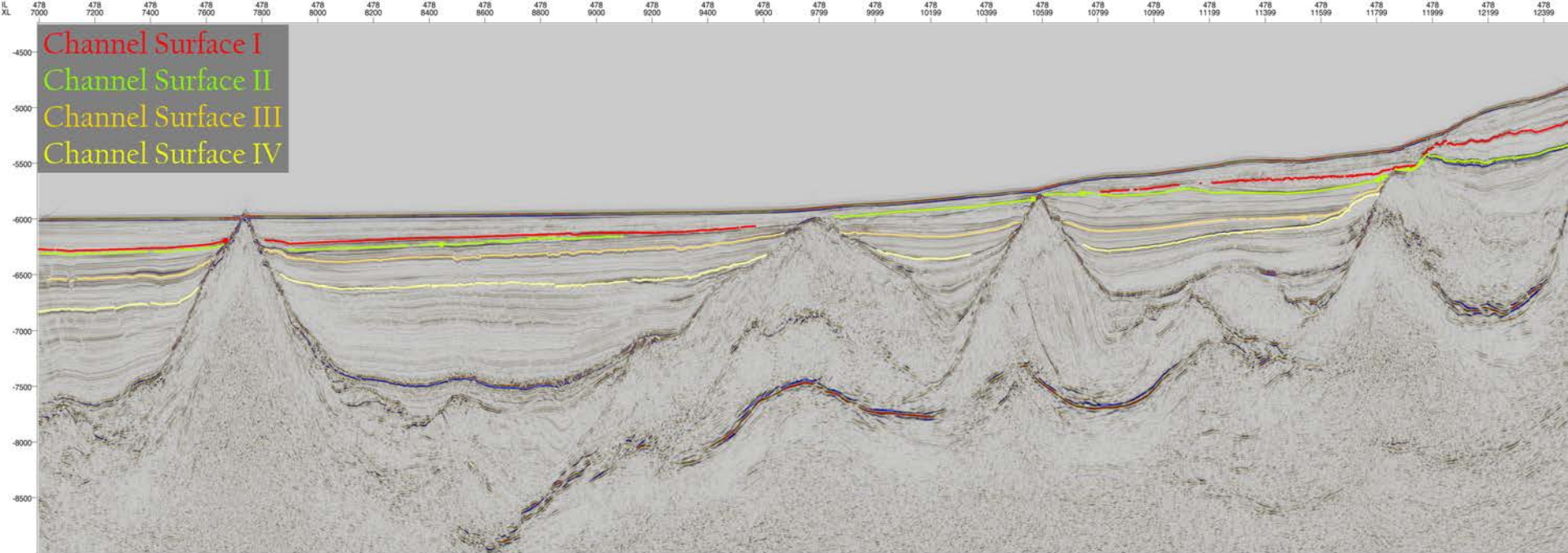
MLSOC  
12/13/2015



**NATURAL  
ENVIRONMENT  
RESEARCH COUNCIL**

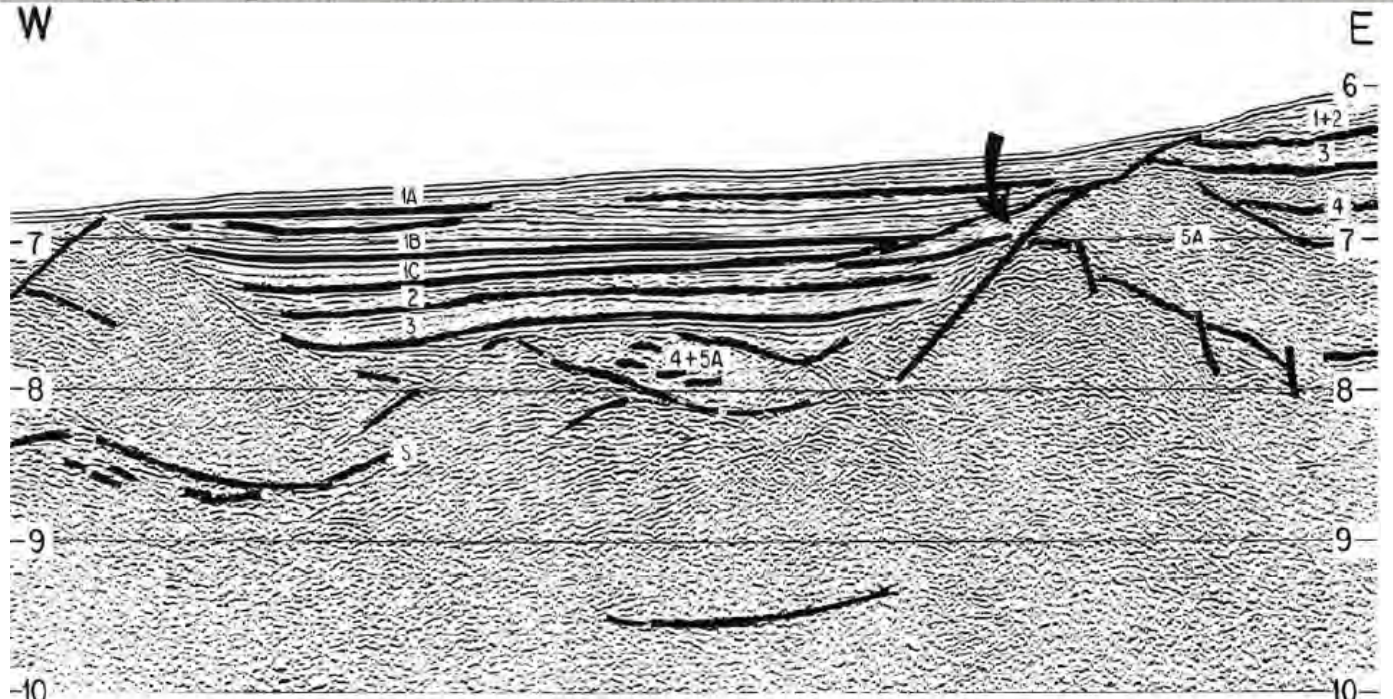






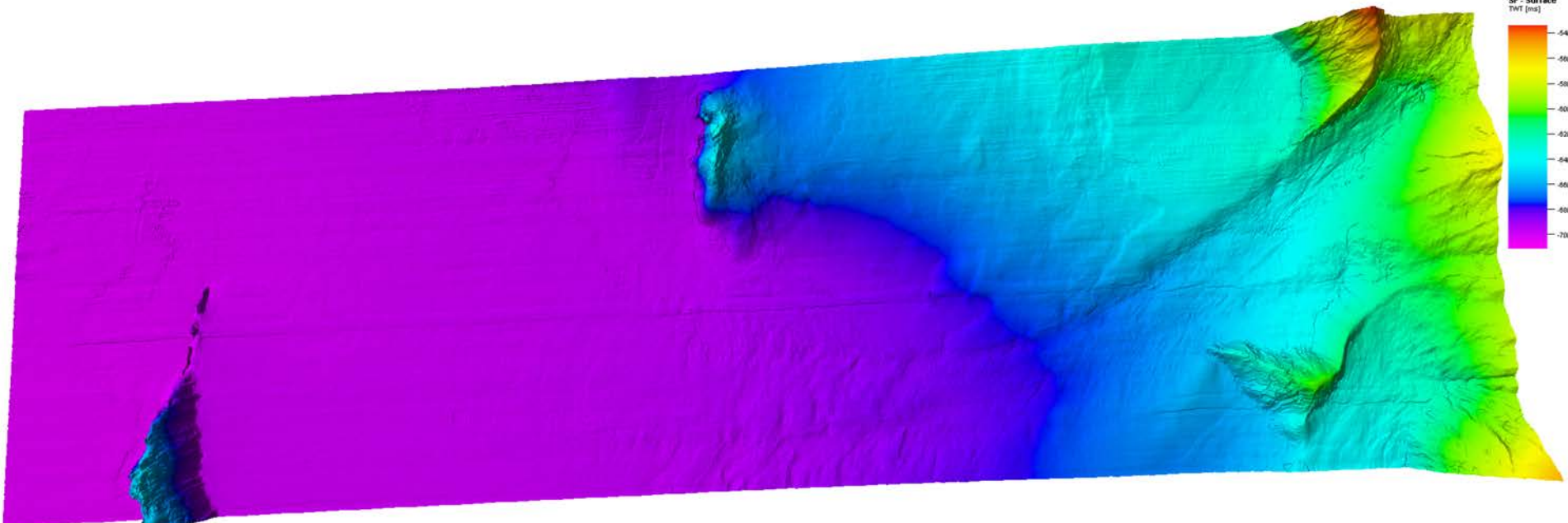
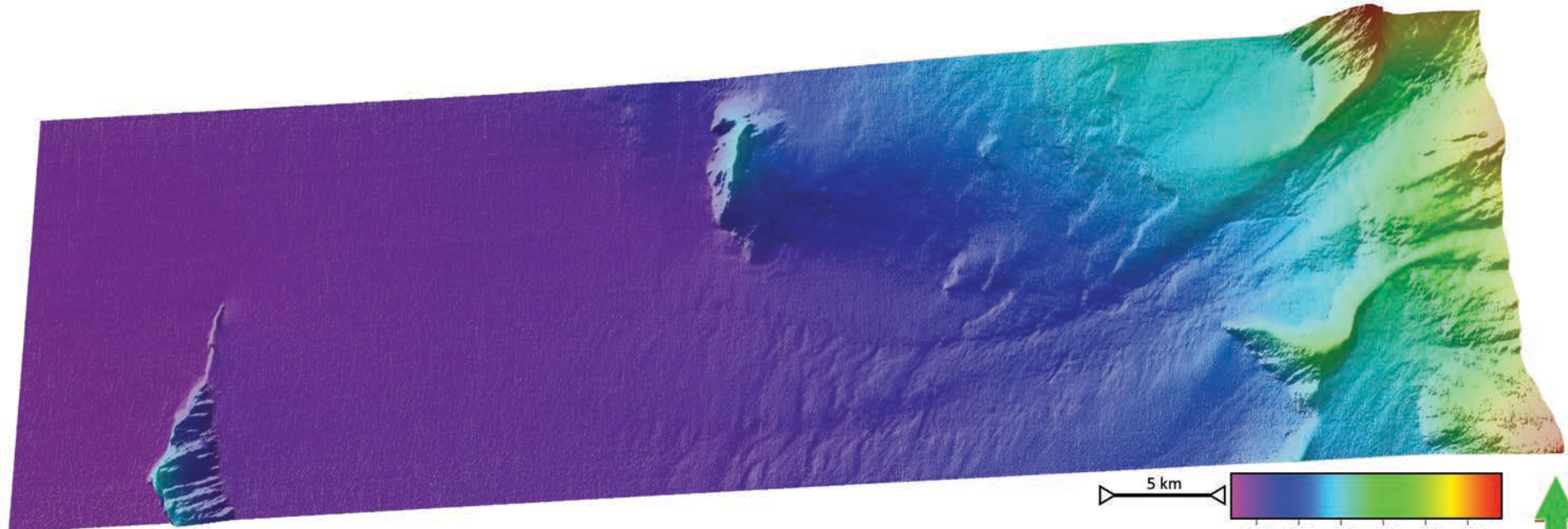
Channel Surface I  
 Channel Surface II  
 Channel Surface III  
 Channel Surface IV

WEST FLANK OF GALICIA BANK this study GPI2 (fig.2) and GPI1 (fig. 8)	
1A -180m	LATE MIOCENE TO RECENT
1B -180m	MIOCENE
1C -220m	OLIGOCENE
2-385m	EOCENE TO SANTONIAN
3-687m	CENOMANIAN TO LATE OR EARLY APTIAN
4-450m	EARLY APTIAN OR LATE BARREMIAN TO HAUTERIVIAN
5A-5 1440m	GP 11 (fig.8) HAUTERIVIAN TO VALANGINIAN
5B=6 400m	BERRIASIAN TO TITHONIAN
5B=7 800m	KIMMERIDGIAN TO OXFORDIAN

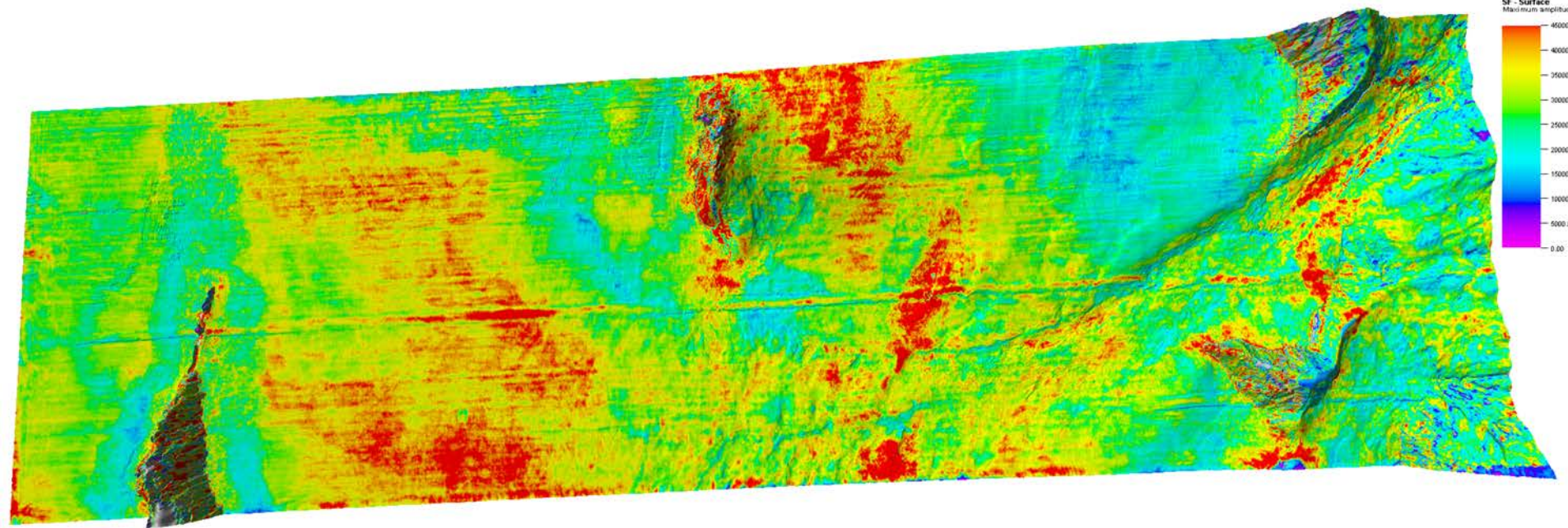
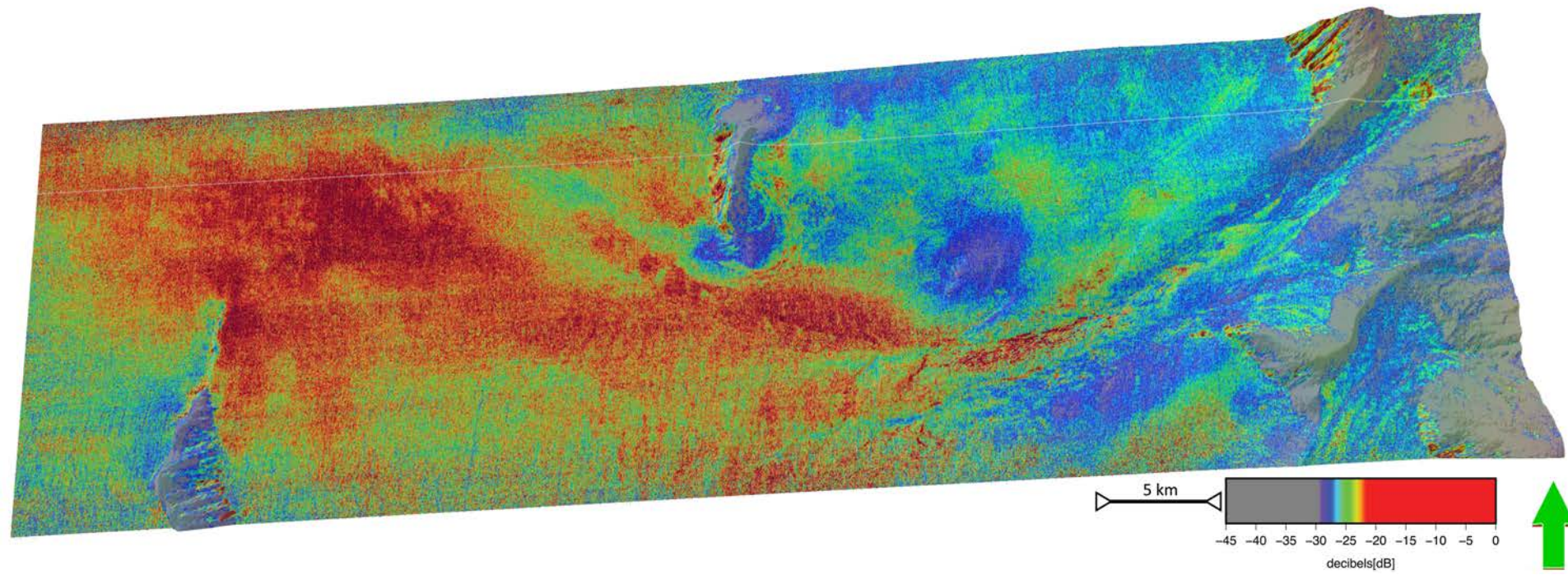


Mauffret, A., and Montadert, L., 1988. Seismic stratigraphy off Galicia, ODP, Sci. Results, 103  
 doi:10.2973/odp.proc.sr.103.119.1988

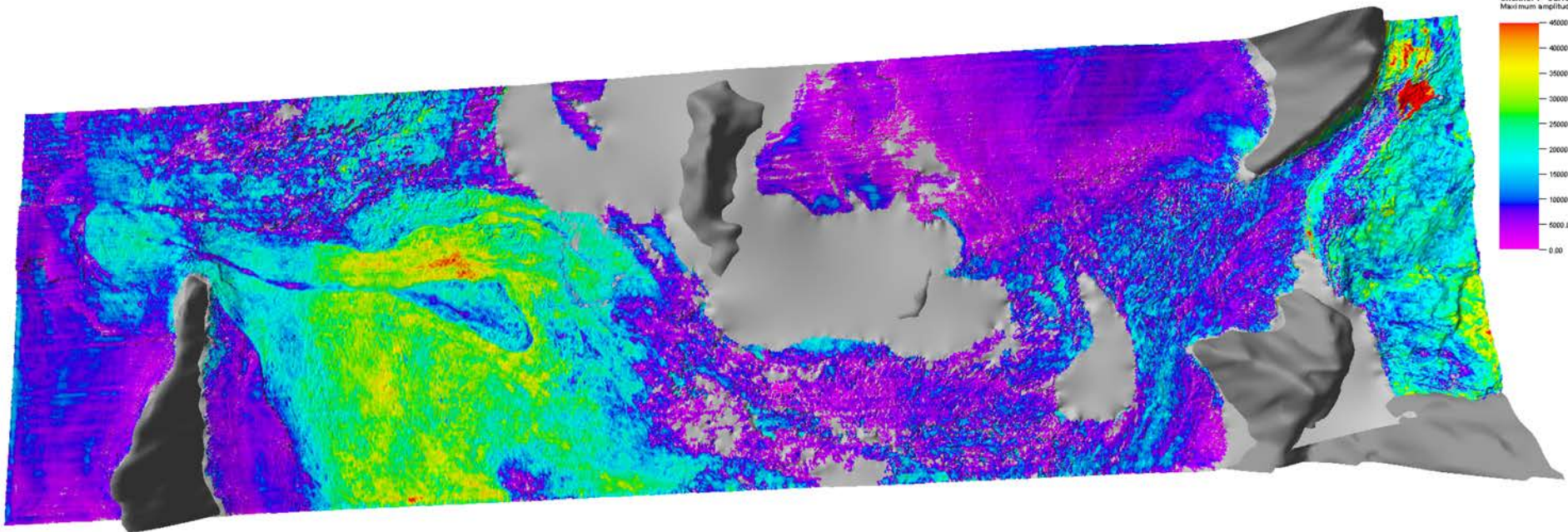
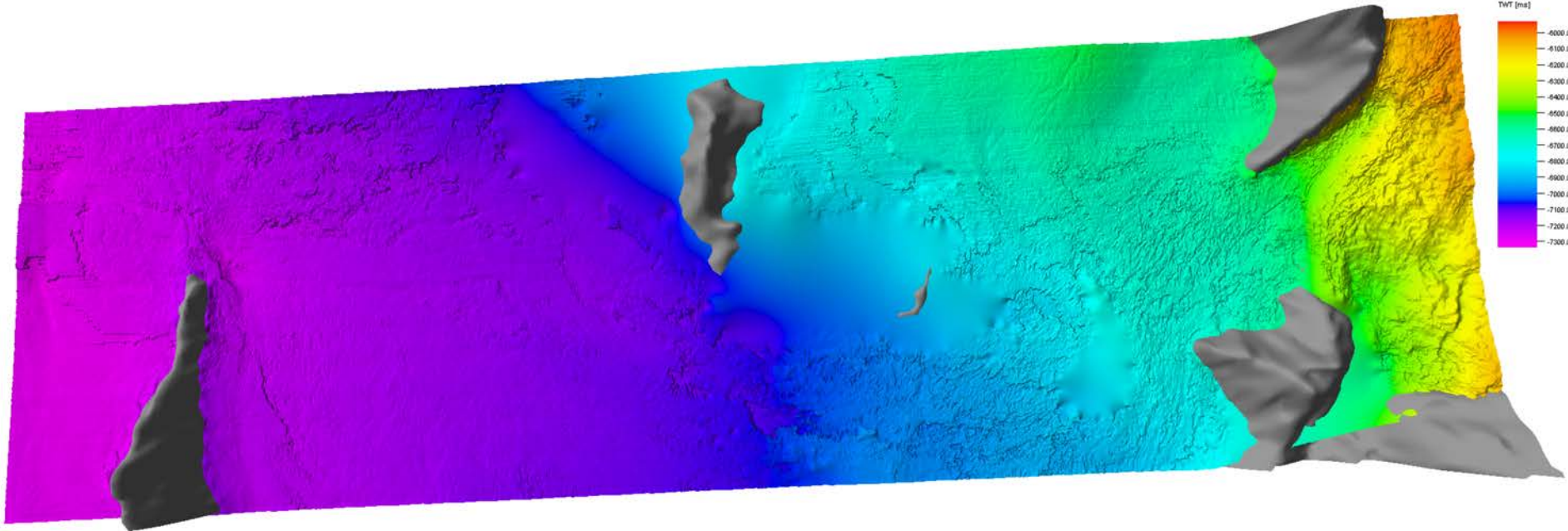




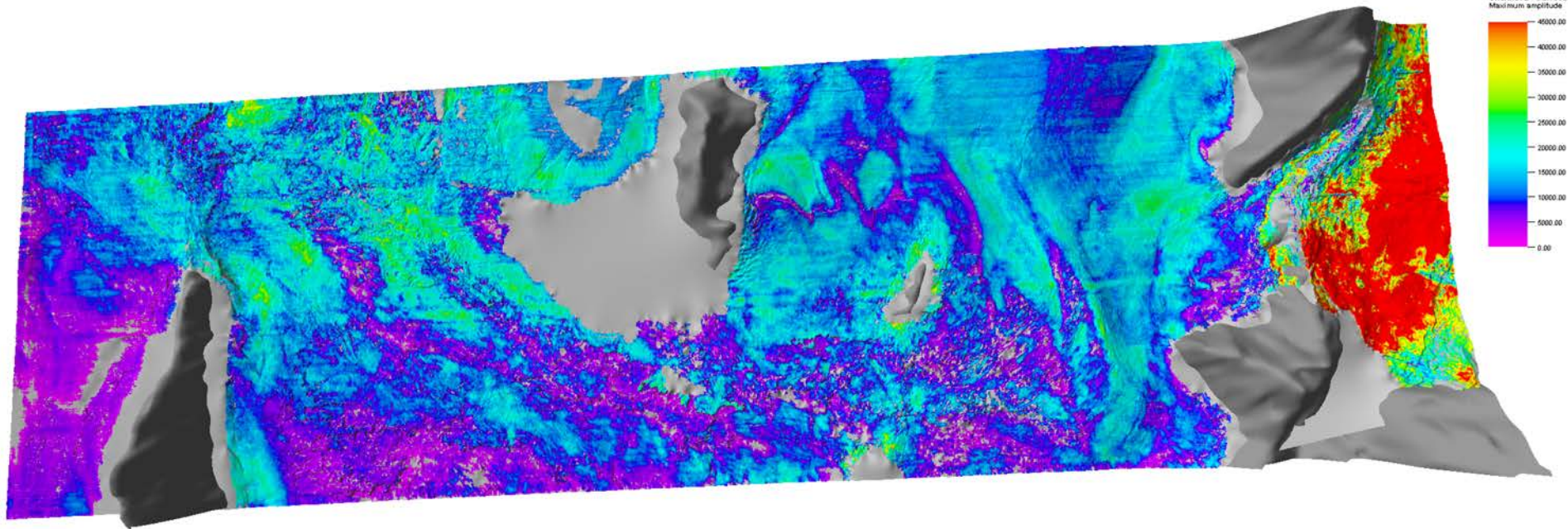
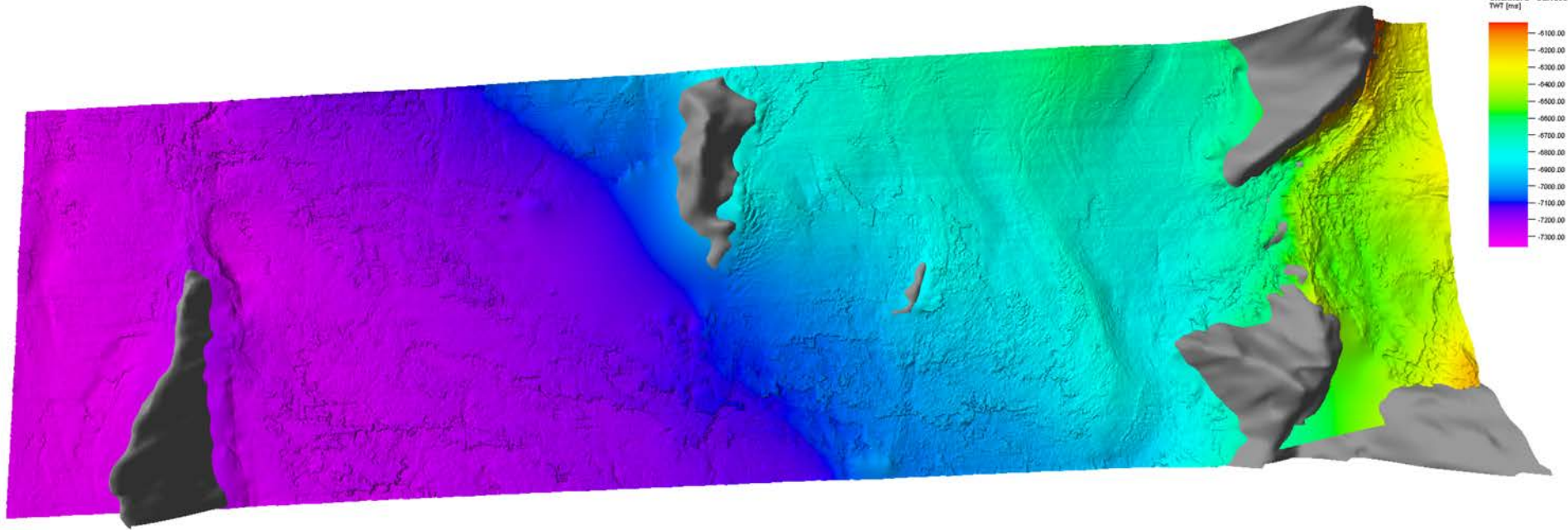




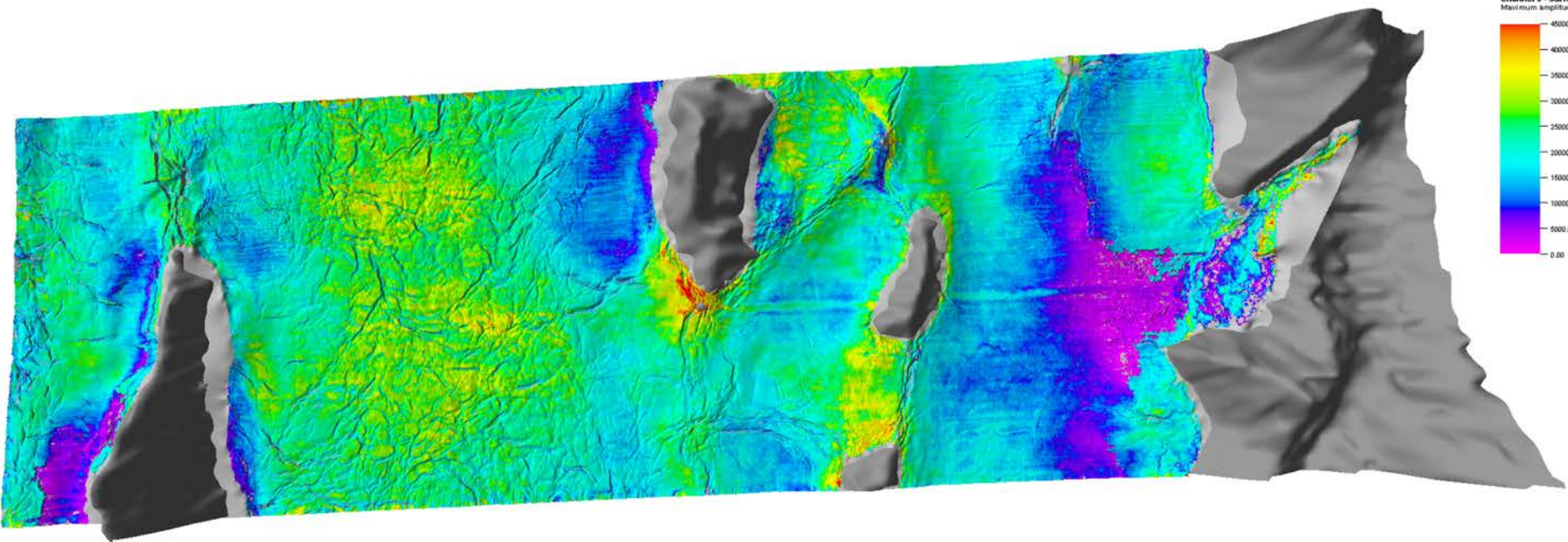
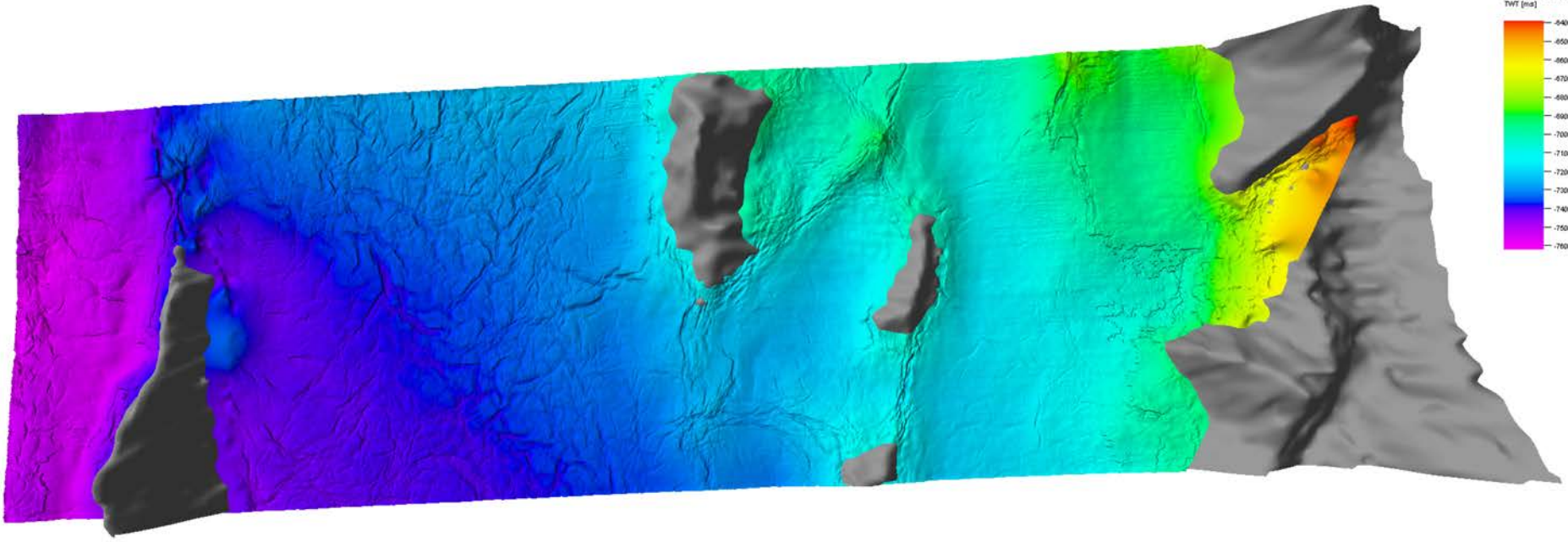




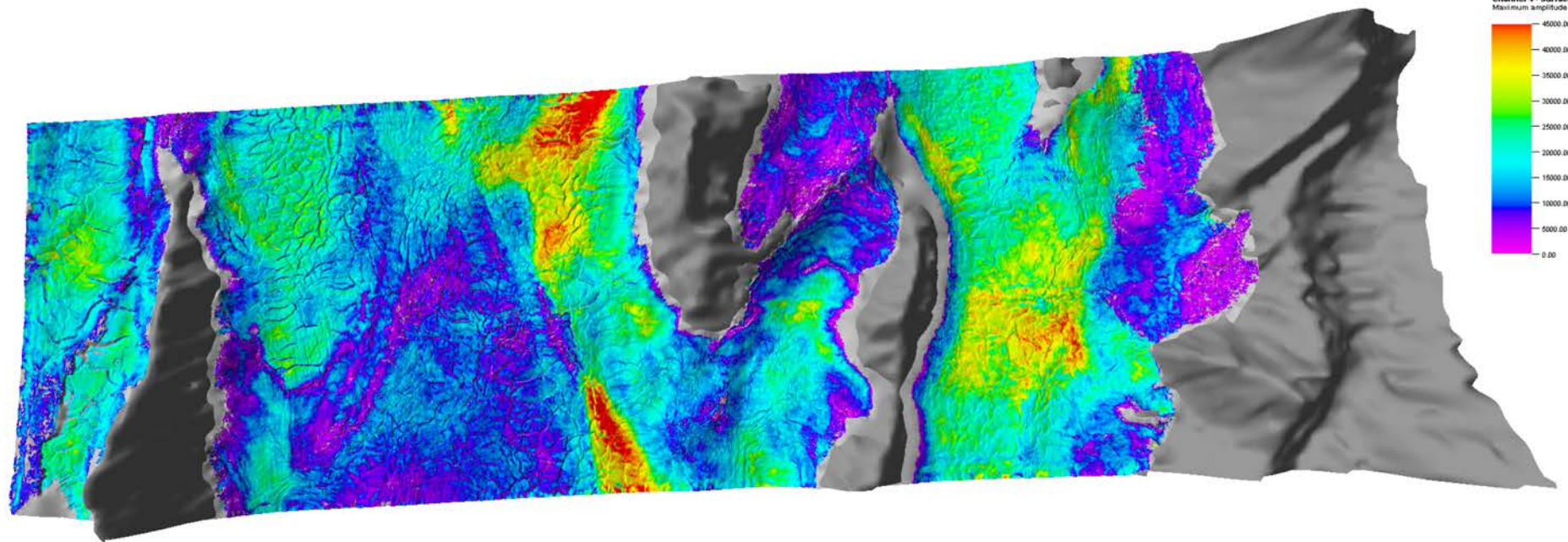
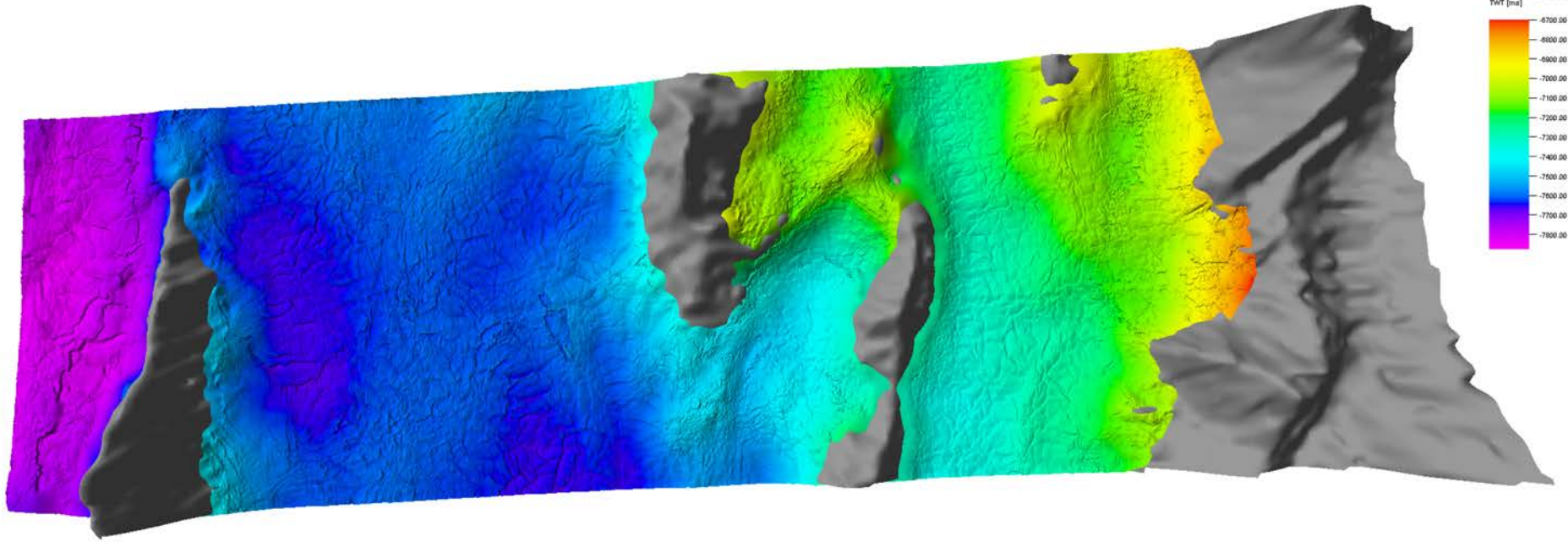














## Marine Sedimentary Records of Climate-Tectonic Interactions II Posters

### Wednesday, December 16<sup>th</sup> 2015; 13:40 - 18:00

Seafloor surface processes and subsurface paleo-channel nonconformities mapped using multi-channel seismic and multi-beam sonar data from the Galicia 3D seismic experiment

James C. Gibson<sup>1</sup>, Donna Shillington<sup>1</sup>, Dale Sawyer<sup>2</sup>, Brian Jordan<sup>3</sup>, Julia Morgan<sup>2</sup>, Cesar Ranero<sup>2</sup>, Tim Reston<sup>4</sup>  
<sup>1</sup>Lamont-Doherty Earth Observatory, Columbia University, New York, NY, USA  
<sup>2</sup>Rice University, Houston, TX, U.S.A.  
<sup>3</sup>CSIC-ICM, Barcelona, Spain  
<sup>4</sup>University of Birmingham, Birmingham, UK



T33D-2970

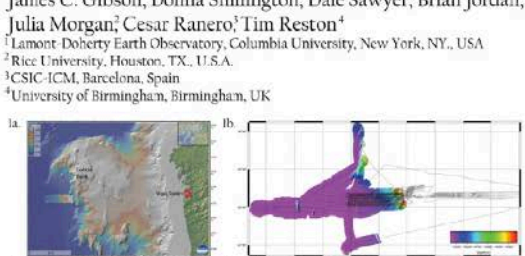


Figure 1a. Overview map of the Galicia 3D seismic experiment. Figure 1b. Overview map of the survey region. The 3D survey is indicated by the color red. The 3D survey track is plotted as black lines. The color data represent swath.

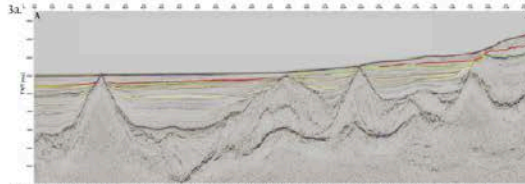


Figure 2a. 23 m MB bathymetry data. Periodic ridges in the west while troughs in the east are visible in the center and to the east. The sediment was within the distal channel have a width of 2 km with a maximum amplitude of 23 m.

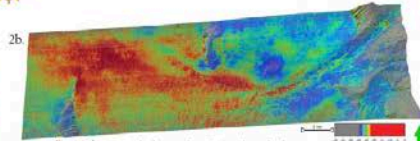


Figure 2b. 23 m MB backscatter data. The data show a bright 'ridge' extending into the abyssal plain. At 12:00:15 this indicates increased reflectivity at the surface shallow sub-surface, which is a function of roughness/irregularities suggesting tectonic differences.



Figure 3b. 25 m emp bin 3D MCS bathymetry data. The data are plotted in two-way travel time and color-coded by depth. The data show a bright 'ridge' extending into the abyssal plain as well as a bright region to the east of the center crestal block, which is not evident in the MB backscatter data. At 50 Hz this indicates increased reflectivity deeper in the shallow sub-surface.

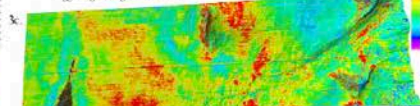


Figure 3c. 25 m emp bin 3D MCS maximum amplitude data. The data show a bright 'ridge' extending into the abyssal plain as well as a bright region to the east of the center crestal block, which is not evident in the MB backscatter data. At 50 Hz this indicates increased reflectivity deeper in the shallow sub-surface.

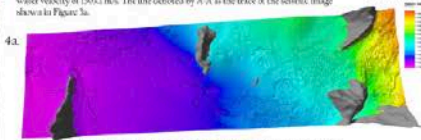


Figure 4a. Channel Surface I. 25 m emp bin MCS data. The data reveal a 400 m deep paleo-canyon mouth by paleo-levies to the south and a crestal block to the north. The basin reflections at the canyon mouth are chaotic, but show a stream line trend indicating seaward flow.

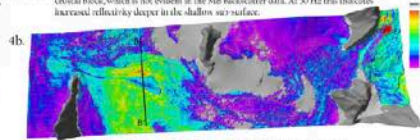


Figure 4b. 25 m emp bin 3D MCS maximum amplitude data. The data reveal a stream line (flowing south) from the canyon mouth. The high amplitude basin reflection indicates possible secondary flow to the west. The line denoted by E-F is the trace of the image shown in Figure 4c.

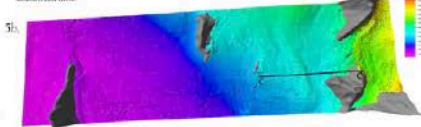


Figure 5b. Channel Surface II. 25 m emp bin MCS data. The data reveal sediment ridges just eastward of the canyon mouth with a maximum amplitude of 200 m rms (300 m). The line denoted by C-C' is the trace of the image shown in Figure 5a.

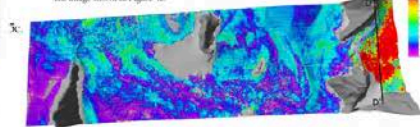


Figure 5c. 25 m emp bin 3D MCS maximum amplitude data. The data show relatively high amplitude on the slopes of the sediment ridges. The very high amplitude reflection to the east lies at the base of a sequence of paleo-levies. The line denoted by D-D' is the trace of the image shown in Figure 5d.

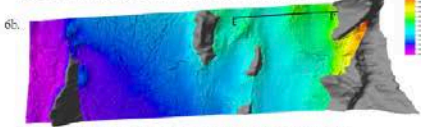


Figure 6b. Channel Surface III. 25 m emp bin MCS data. The data reveal a trace of the canyon opening into a smooth basin with exception of compression deformation around buried ridges, along with a broad polygonal faulting within the basin to the east of Pendote Ridge. The line denoted by E-E' is the trace of the image shown in Figure 6c.

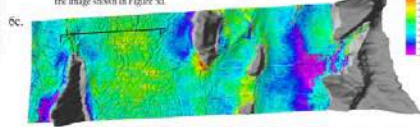


Figure 6c. 25 m emp bin 3D MCS maximum amplitude data. The data show high amplitude surrounding the crestal blocks as well as pooling in the basin to the east of Pendote Ridge. The low amplitude region southeast of the canyon mouth may be related to reflection divergence. The line denoted by F-F' is the trace of the image shown in Figure 6d.

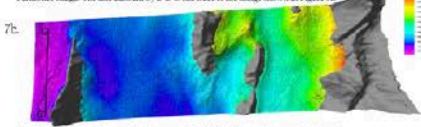


Figure 7b. Channel Surface IV. 25 m emp bin 3D MCS data. The data reveal adjacent compressive deformation around the ridges as well as an increase in the frequency of the polygonal faults. The line denoted by G-G' is the trace of the image shown in Figure 7c.

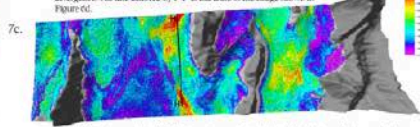


Figure 7c. 25 m emp bin 3D MCS maximum amplitude data. The data show high amplitudes outward of the canyon mouth with a 'fan' like geometry. The high amplitudes to the west follow the strike of the crestal blocks. The line denoted by H-H' is the trace of the image shown in Figure 7d.



Figure 2c. The inside 400 m nadir region was cut in order to enhance the 'ridge' and to equally high amplitude reflections. The backscatter data were then low-pass filtered. This resulted in 23 m bathymetry and 0 m backscatter (darker).



Figure 3d. Data processing was performed by Repet and included low cut filter, swell noise filter, linear 3000 attenuation, surface consistent amplitude correction, time deconvolving, 3D regularization. The data were then pre-stack time migrated.

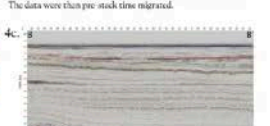


Figure 4c. Xline 87/4 showing Channel Surface I across the high amplitude basin reflection. The amplitude decreases from inline 410-400.

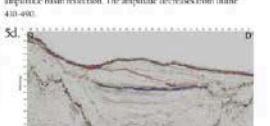


Figure 5d. Xline 107/3 showing a 'V' of Channel Surfaces I (red) and II (blue). The data show sediment walls parallel to the strike of the paleo-levies (inline 400-600).



Figure 6d. Xline 70/0 showing Channel Surface III across compression deformation in the form of polygonal faults in the basin and grabens above the buried Pendote Ridge (line 7000-7300).

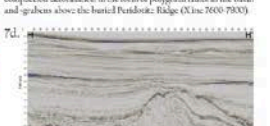


Figure 7d. Xline 0166 showing Channel Surface IV across high amplitude basin reflections bounding a buried crestal block. The data also reveal faults that extend shallow in the section suggesting recent fault growth (inline 440-480).

Abstract:

In this study we use geophysical methods, stratigraphic relationships and chrono-stratigraphy to investigate the basin evolution in order to further constrain paleo-climate (PC) and associated tectonic/climate processes. A 3D seismic and MB PC survey was mapped in 3D multi-channel system (MCS) data and compared with multi-beam (MB) bathymetry data to investigate the evolution of the Galicia 3D survey within the E-V basin (C. Lopez 2010). The MCS data were collected using 4 m track spacing equal to 200 m resulting in 25 m x 25 m coverage and post beam width of 47 km x 20 km. The MB data were collected with an average track width of 400 m with a maximum swath width of 43 km resulting in 220 m overlap along track 25 m bathymetry and 40 m backscatter grid. The PC below the onset of a sedimentary sequence in the Galicia 3D survey data and at present day sediments, they are bounded by both blocks to the west and paleo-levies to the east (Lopez 2010). From MB data results, the new marine PC is Jan-March stage. Four PC are traced from basin to microdeformations. Several of the PC conformities are correlated with periodic interglacial Pleistocene or compressed Pleistocene stages in the basin. However, the PC conformity which has been traced from previously interglacial basins to the Pleistocene stage conformities are the result of a significant change in the basin evolution. The MB MCS data were used to compare the extent of recent processes (i.e., Pleistocene glacial-interglacial) with the reconstruction by mapping the surface shallow sub-surface (i.e., bathymetry).

Methods:

In order to test the three surface and related stratigraphic block based basin reconstructions the basin was traced at intervals of 30 m and 200 m across the survey range (2000 m by 2000 m). While tracking the surface reconstruction, relationships as well as faulting, compression, and erosion were taken into account when reconstructing the basin evolution. The resulting basin was then used to compare the extent of recent processes (i.e., Pleistocene glacial-interglacial) with the reconstruction by mapping the surface shallow sub-surface (i.e., bathymetry).

Conclusion:

The channel surface reveal a broad range of high amplitude features across the basin and a different stratigraphic levels. The current surface reflectivity indicates a relatively more progradational distribution of high amplitude possibly associated with flow draping and burial of the first generation sediments and subsequent deposition of the more gradual sediments on the top of later. Additionally the surface reveal multiple compression deformation as well as a variety of faulting patterns. Suggesting that the primary control on both sediment distribution and subsequent faulting in the studied block geometry. The same area will be further use the surface in order to achieve a higher resolution level, which will be data better interpretation. Once the surface are complete will be further use the surface in order to achieve a higher resolution level, which will be data better interpretation. Once the surface are complete will be further use the surface in order to achieve a higher resolution level, which will be data better interpretation.

Contact: jgibson@ldeo.columbia.edu

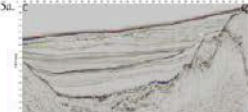


Figure 3a. Xline 479 showing the buried crustal block bounded by the channels to the east and the Pendote Ridge to the west. The Channel Surfaces I (red), II (green), III (cyan), IV (yellow).

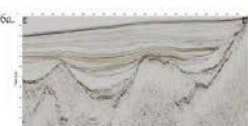


Figure 3b. Xline 108 showing Channel Surface II across a buried sediment ridge/possible buried channel (Xline 120-150).



Figure 5a. Xline 788 showing Channel Surface III across compression deformation in the form of polygonal faults in the basin and grabens above the buried Pendote Ridge (Xline 10300-10350; 10310-10340).

Contact: jgibson@ldeo.columbia.edu